

## Hydrodesulfurization Activity and Defect Structure of Co-Mo Sulfide Catalyst

P. R. WENTRCEK AND H. WISE

*Solid State Catalysis Laboratory, Stanford Research Institute, Menlo Park, California 94025*

Received December 2, 1976; revised August 31, 1977

To elucidate the effect of cobalt on the hydrodesulfurization (HDS) activity of molybdenum-sulfide catalysts, experimental studies have been made with a single crystal of MoS<sub>2</sub> doped with Co<sup>2+</sup>. From electrical conductance and Hall coefficient measurements it was determined that the addition of Co<sup>2+</sup> (<0.1 mole%) caused a change from n-type to p-type conductivity on the MoS<sub>2</sub>. Without the foreign cation additive, the MoS<sub>2</sub> catalyst exhibited a range of catalytic properties for the HDS of butyl mercaptan which varied with the density of S<sup>2-</sup> anion vacancies. But the Co<sup>2+</sup>-doped catalyst was found to be (1) stable to sulfiding or reduction on exposure to reactants, (2) catalytically active for the production of butane and hydrogen sulfide, and (3) relatively constant for reactant conversion and product distribution. Kinetic analysis showed that the HDS activity is proportional to hole carrier density.

### INTRODUCTION

The demand for low-sulfur fuels has placed renewed emphasis on the development of efficient hydrodesulfurization (HDS) catalysts for industrial applications. Of special importance are the alumina-supported catalysts containing molybdenum or tungsten compounds with cobalt and nickel as additives. In the interpretation of the role played by the additives, several solid-state models are currently under discussion. One involves the formation of Mo<sup>3+</sup> and W<sup>3+</sup> cations in the sulfide crystallite adjacent to vacancies located at crystal edges and promoted by intercalation of the additive ions (1). The other model is based on the observation that Co<sup>2+</sup> tends to form a cobalt aluminate surface spinel and tends to stabilize the Mo<sup>4+</sup> sites octahedrally coordinated in a layer on the surface of the support (2). Also the intercalation of Co<sup>2+</sup> in the molybdenum sulfide layer structure has been suggested

in an interpretation of the promoting effect of cobalt (3). To examine in greater detail the role played by cobalt addition to MoS<sub>2</sub> we have used the experimental approach previously described in which a single crystal of molybdenite is employed as the catalyst (4) for HDS of a sulfur-containing compound, such as butyl mercaptan. Powdered molybdenum sulfide has been shown to exhibit HDS properties similar to those of sulfided molybdenum-oxide catalyst (5). However, the use of a single crystal allows simultaneous measurement of electronic and chemical properties of the catalyst during reaction.

In the case of MoS<sub>2</sub>, measurement of electronic properties is of particular interest since this compound semiconductor can exhibit both excess and defect conductivity (n and p type), and deviations from stoichiometric composition (Mo<sup>4+</sup>/S<sup>2-</sup>  $\leq \frac{1}{2}$ ) can be established from electrical properties. Similarly "controlled conductivity,"

as suggested by Verwey (6), can result from the incorporation of foreign ions. Thus the introduction of  $\text{Co}^{2+}$  or  $\text{S}^{2-}$  into  $\text{MoS}_2$  will favor the formation of cation vacancies and hole carriers (p-type conductivity). On the other hand, the removal of  $\text{S}^{2-}$  anions from  $\text{MoS}_2$  will lead to electron injection (n-type conductivity) and the formation of anion vacancies. Thus the electrical conductivity and the type of electronic majority carrier in  $\text{MoS}_2$  can be controlled by the addition or removal of "impurity" ions. The objective of this research is to relate the defect structure of  $\text{MoS}_2$  to its catalytic properties as manifested in the HDS of butylmercaptan.

#### EXPERIMENTAL DETAILS

##### *Catalyst*

A small single crystal (typical dimensions,  $1 \times 1 \times 0.06$  cm) was cut from a large crystal of the naturally occurring mineral molybdenite<sup>1</sup> (hexagonal crystal structure C7). It was mounted in a quartz reactor provided with four glass-coated platinum leadthroughs for electrical contact with the crystal and electrical conductivity measurements by the four-probe technique (7). Hall coefficient determinations (8) at room temperature demonstrated n-type conductivity for the freshly cleaved crystal of molybdenite. The introduction of  $\text{Co}^{2+}$  was achieved by dipping the crystal in an aqueous solution of  $\text{Co}(\text{NO}_3)_2$  (0.1 M) followed by evaporation of the solvent in a vacuum oven at 325 K. Subsequently, the crystal was placed in the quartz reactor and heated in a helium stream to 900 K before exposure to a hydrogen stream at 880 K. Incorporation of  $\text{Co}^{2+}$  into the crystal was facilitated by heating the doped crystal in He for various time intervals. The doping process was monitored by electrical conductivity and Hall coefficient studies (Table 1). Based on

<sup>1</sup> The molybdenite crystal was kindly provided by the Climax Molybdenum Company of Michigan.

TABLE 1  
Properties of  $\text{Co}^{2+}$ -Doped  $\text{MoS}_2$  Crystal

Treatment	Electrical conductivity at 300 K (mho · cm <sup>-1</sup> )	Electronic majority carrier
Before deposition of $\text{Co}^{2+}$	0.17	n Type <sup>a</sup>
After deposition of $\text{Co}^{2+}$ and heating at 900 K for 18 hr in He	0.42	p Type <sup>b</sup>
After reduction in $\text{H}_2$ at 880 K	0.35	p Type <sup>a</sup>
After exposure to $\text{H}_2\text{S}$	0.47	p Type <sup>b</sup>

<sup>a</sup> Based on Hall coefficient measurement.

<sup>b</sup> Based on direction of conductivity change on exposure to butyl mercaptan or hydrogen sulfide (4).

the electrical conductivity data we estimate a doping level of 10 to 100 ppm.

##### *Apparatus*

The reactor housing the catalyst crystal was so designed to allow operation in the pulse mode or under continuous flow conditions. In the pulse mode a stream of hydrogen gas (volume flow rate = 2 ml/sec NTP) was passed continuously through the reactor (36 ml in volume) housing the catalyst crystal and surrounded by a furnace maintained at a specified temperature. Into this stream of hydrogen, pulses of gaseous reactant ( $\text{C}_4\text{H}_9\text{SH}$ ) could be injected. Liquid butyl mercaptan was vaporized in a special device employing as a heating element a porcelain-encased wire resistor (Ohmite, 10 watt) covered with several layers of glass fiber. The liquid was displaced onto this heater from a mechanically driven syringe and vaporized into a carrier stream of hydrogen. By adjusting the liquid feed rate and the carrier gas flow rate, we were able to obtain specified concentrations of reactant. In most of the experiments the volumetric ratio of  $\text{H}_2/\text{C}_4\text{H}_9\text{SH}$  ranged from 70 to 80. In a typical pulse experiment an aliquot of the pre-vaporized gas mixture was injected into the reactor. After passage over the catalyst it entered the gc column for product analysis. Provisions were made to bypass

the reactor for sample analysis of the inlet compositions. For chromatographic analysis of butenes, butane, hydrogen sulfide, and butyl mercaptan, a temperature programmed Poropak R column was employed.

Under continuous flow conditions the gas mixture of hydrogen and butyl mercaptan (volume ratio = 75/1) was passed through the reactor at a volumetric flow rate of 2 ml/sec (NTP). After passage over the catalyst, an aliquot of the product stream could be subjected to gc analysis. The experimental configuration permitted sampling of the reactor inlet and outlet gas mixtures.

For quantitative analysis of the reactant product distribution, the gc apparatus was calibrated for each component. Also for catalyst pretreatment, a special line was provided to admit H<sub>2</sub>, He, or H<sub>2</sub>S to the reactor with a bypass of the gc system.

#### EXPERIMENTAL RESULTS

Changes in the electrical properties of the catalyst crystal could be monitored during both the pretreatment procedure (H<sub>2</sub>, or H<sub>2</sub>S, or Co<sup>2+</sup> doping) and the catalytic experiments. For initial activation of the catalyst for HDS the undoped molybdenum sulfide was reduced in hydrogen at 880 K. The electrical measurements demonstrated sulfur removal accompanied by an increase in conductivity due to electron (e) injection in accordance with:

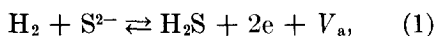


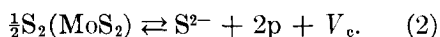
TABLE 2  
HDS of Butyl Mercaptan<sup>a</sup> Catalyzed by  
Molybdenum Sulfide at 700 K

Experiments	Electrical conductivity <sup>b</sup> (mho · cm <sup>-1</sup> ) (n type)	Total exposure (min)	Conversion (vol%)		C <sup>2-</sup> /ΣC <sub>4</sub> (vol%)
			Initial	Final	
1	2.1	190	73	67	50
2	2.9	180	53	40	45
3	3.25	150	10	6	70

<sup>a</sup> H<sub>2</sub>/C<sub>4</sub>H<sub>9</sub>SH = 77 (by volume).

<sup>b</sup> After various extents of reduction by H<sub>2</sub> at 880 K.

where V<sub>a</sub> represents an anion vacancy. Just the opposite electrical effect was brought about by treatment of a sulfur-deficient catalyst (Mo<sup>4+</sup>/S<sup>2-</sup> > ½) in a H<sub>2</sub>S/H<sub>2</sub> environment at 880 K, i.e., establishment of a specified sulfur vapor pressure. Under these conditions a decrease in electron density was observed due to the reverse of reaction (1). However, once the stoichiometric composition was reached, further introduction of sulfur ions led to a conductivity increase caused by electronic hole carriers, in accordance with:



By these pretreatment procedures the defect structure of the catalyst could be adjusted and its effect on catalytic activity examined, since the layer structure of hexagonal MoS<sub>2</sub> favors rapid transport of ionic species within the lattice and equilibrium of bulk and surface properties. The extent of preexposure of the catalyst to H<sub>2</sub> (progressive extent of S<sup>2-</sup> removal) had a pronounced effect on catalytic activity, as shown by the results presented in Table 2 in which we list the degree of conversion, the product distribution, and the electrical conductivity of the catalyst. The conversion data indicate that a catalyst of relatively low conductivity, representative of few S<sup>2-</sup> ion vacancies, exhibits high and prolonged activity for HDS of C<sub>4</sub>H<sub>9</sub>SH over several hours of operation at 700 K. However, an increase in S<sup>2-</sup> ion vacancies, brought about by pretreatment of the catalyst in H<sub>2</sub> at 920 K, resulted in a marked decrease in conversion rate accompanied by a higher proportion of butene in the product stream (Table 2). In addition, a gradual decay in catalyst activity with exposure time was observed, particularly for the catalyst highly deficient in S<sup>2-</sup> anions (high n-type conductivity).

Variations of the hydrogen concentration in the feed stream demonstrated a marked influence of the H<sub>2</sub>/C<sub>4</sub>H<sub>9</sub>SH ratio on conversion rate, product distribution, and

TABLE 3

Effect of Hydrogen on HDS of Butyl Mercaptan Catalyzed by Molybdenum Sulfide<sup>a</sup> at 700 K

H <sub>2</sub> /C <sub>4</sub> H <sub>9</sub> SH (by vol)	Total exposure (min)	Conversion (vol%)		C <sub>4</sub> <sup>2-</sup> /ΣC <sub>4</sub> (vol%)	ΣC <sub>4</sub> /H <sub>2</sub> S (by vol)
		Initial	Final		
77	190	73	67	50	1.0
15	210	20	13	62	1.45
3	205	5	2	70	1.6
0	90	0.7	0.1	—	—

<sup>a</sup> Initial electrical conductivity = 2.1 mho · cm<sup>-1</sup> (n type).

activity decay (Table 3). Of interest is the relative growth of olefinic C<sub>4</sub> compounds (C<sub>4</sub><sup>2-</sup>) relative to butane (C<sub>4</sub>) with lowering of the H<sub>2</sub>/C<sub>4</sub>H<sub>9</sub>SH ratio. This change in distribution of the hydrogen products was accompanied by retention of sulfur on the catalyst surface, as evidenced by the increase in the Σ C<sub>4</sub>/H<sub>2</sub>S ratio (Table 3).

For the Co<sup>2+</sup>-doped catalyst the fractional conversion of butyl mercaptan over a range of temperatures is summarized in Fig. 1. Contrary to the undoped catalyst, pretreatment in H<sub>2</sub>S/H<sub>2</sub> mixtures ( $\sigma_{700} = 0.44 \text{ mho} \cdot \text{cm}^{-1}$ ) and pretreatment in H<sub>2</sub> ( $\sigma_{700} = 0.38 \text{ mho} \cdot \text{cm}^{-1}$ ), under conditions similar to those employed for the undoped catalyst, causes only small changes

in electronic and catalytic properties (Table 4). In addition, the HDS of C<sub>4</sub>H<sub>9</sub>SH yields only butane as a hydrocarbon product and the ratio of C<sub>4</sub>H<sub>10</sub>/H<sub>2</sub>S remains close to unity. These observations are in marked contrast to the n-type material, where the introduction of S<sup>2-</sup> ion vacancies into MoS<sub>2</sub> (high n-type conductivity) causes a marked decrease in total conversion and the formation of butene as the predominant product (Table 2).

## DISCUSSION

The MoS<sub>2</sub>/Co<sup>2+</sup> catalyst exhibits catalytic properties that are markedly different from those observed in the absence of cobalt additive. Most striking is the ob-

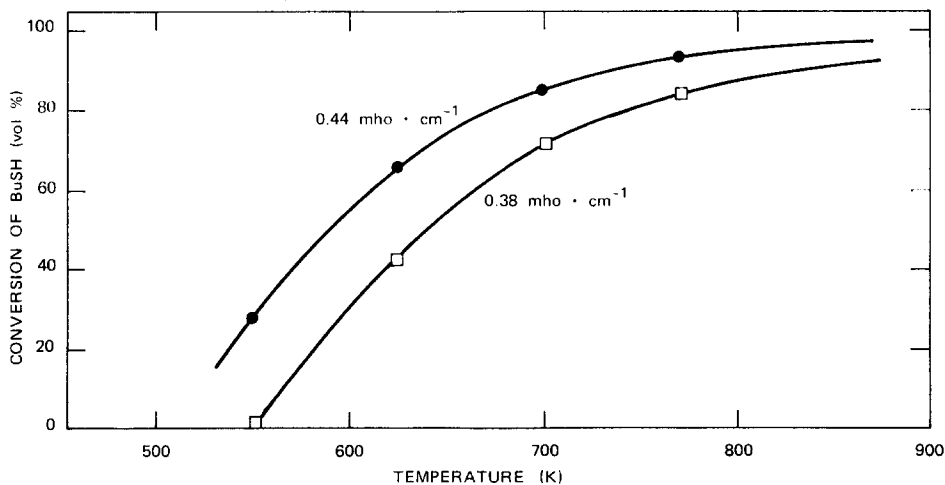


FIG. 1. HDS activity of MoS<sub>2</sub>/Co catalyst (H<sub>2</sub>/C<sub>4</sub>H<sub>9</sub>SH = 77): (●) after exposure to H<sub>2</sub>S/H<sub>2</sub> mixture (cf. Table 1), and (□) after exposure to H<sub>2</sub> (cf. Table 1).

TABLE 4  
HDS Activity and Product Distribution at 700 K\*

Catalyst	Electrical conductivity (mho · cm <sup>-1</sup> )	Conversion (vol%)	Butane specificity (vol%)
MoS <sub>2</sub>	2.1	70	50
	3.3	8	30
MoS <sub>2</sub> (Co <sup>2+</sup> )	0.44	87	100
	0.38	68	100

\* H<sub>2</sub>/C<sub>4</sub>H<sub>9</sub>SH = 77 vol%.

ervation that during prolonged exposure to reactant feed (H<sub>2</sub>/C<sub>4</sub>H<sub>9</sub>SH = 77 vol%) the cobalt-promoted catalyst exhibits relatively constant activity in terms of total conversion and product distribution. Second, the products formed from the HDS reaction of butyl mercaptan are butane and H<sub>2</sub>S, without any measurable amounts of butene. The formation of alkanes may result from rapid olefin hydrogenation (9), a reaction strongly catalyzed by the MoS<sub>2</sub>/Co<sup>2+</sup>. Third, the catalyst defect structure remains stable under the experimental conditions, i.e., no changes in conductivity occur during prolonged exposure to reactant gas, in contrast to our observations on an unpromoted sulfur-deficient catalyst sample.

Kinetic measurements indicate that the HDS reaction catalyzed by MoS<sub>2</sub>/Co<sup>2+</sup> is of first order with respect to C<sub>4</sub>H<sub>9</sub>SH in the presence of an excess of hydrogen [40 < (H<sub>2</sub>/C<sub>4</sub>H<sub>9</sub>SH) < 80], as observed for a number of S compounds (3, 10-12). Also from the variation in fractional conversion with reaction temperature, on the basis of a first-order analysis, we calculate an activation energy of 12 ± 1 kcal/mole.

To obtain a better understanding of the role of electronic carriers in HDS catalysis, we can calculate from the conductivity data the absolute electron or hole densities with the aid of published mobility data (13, 14). Although the mobilities for holes are not as well established as those for electrons, the general trend of the HDS rate data as a function of carrier type and density is of interest. As shown in Fig. 2, an increase in

electron carriers reduces catalyst activity, while an increase in hole carriers enhances the HDS rate. In this semilogarithmic correlation the (BuSH)<sub>i</sub>/(BuSH)<sub>f</sub> represents the ratio of the initial to final concentrations of butyl mercaptan, whose logarithm is proportional to the first-order rate constant. Therefore the HDS reaction rate obeys a rate law of the form  $-d(\text{BuSH})/dt = k_p(\text{BuSH})(n_p) = k_e(\text{BuSH})/n_e$ , with  $n_p$  indicating the hole density for the p-type MoS<sub>2</sub>/Co<sup>2+</sup>,  $n_e$  the electron density for the n-type MoS<sub>2</sub> catalyst, and  $k_p$  and  $k_e$  the appropriate rate constants.

For the relative distribution of electronic carriers one finds under equilibrium conditions:

$$K_i = n_e n_p = N_c N_v e^{-E_i/kT}, \quad (3)$$

where  $K_i$  is the equilibrium constant,  $n_e$  and  $n_p$  the electron and hole densities,  $N_c$  the number of available states in the conduction band,  $N_v$  that in the valence band, and  $E_i$  is the band-gap energy ( $E_c - E_v$ ). In view of the fact that  $n_p = K_i/n_e$ , it is apparent that the functional relationship between  $n_e$  and  $n_p$  exhibited by the data in Fig. 2 is to be expected on the basis of solid-state theory.

To relate the conductivity data to the defect structure of the solid, one needs to consider the interactions at the gas-solid interface that lead to the formation of vacancies and electronic charge carriers. The vacancies perturb the local potential in the solid and give rise to localized electron energy levels located between the S<sup>2-</sup> band (filled valence band,  $E_v$ ) and the Mo<sup>4+</sup> band (empty conduction band,  $E_c$ ). Since the anion vacancy  $V_a$  can bind an electron, a localized level  $V_a^-$  will be found in the band gap. This energy level lies close to the valence band, and most likely in close proximity to the energy level associated with Co<sup>2+</sup> in Co-doped molybdenum sulfide. Thus the electronic properties of n-type molybdenite are affected qualitatively in an analogous way by the addition

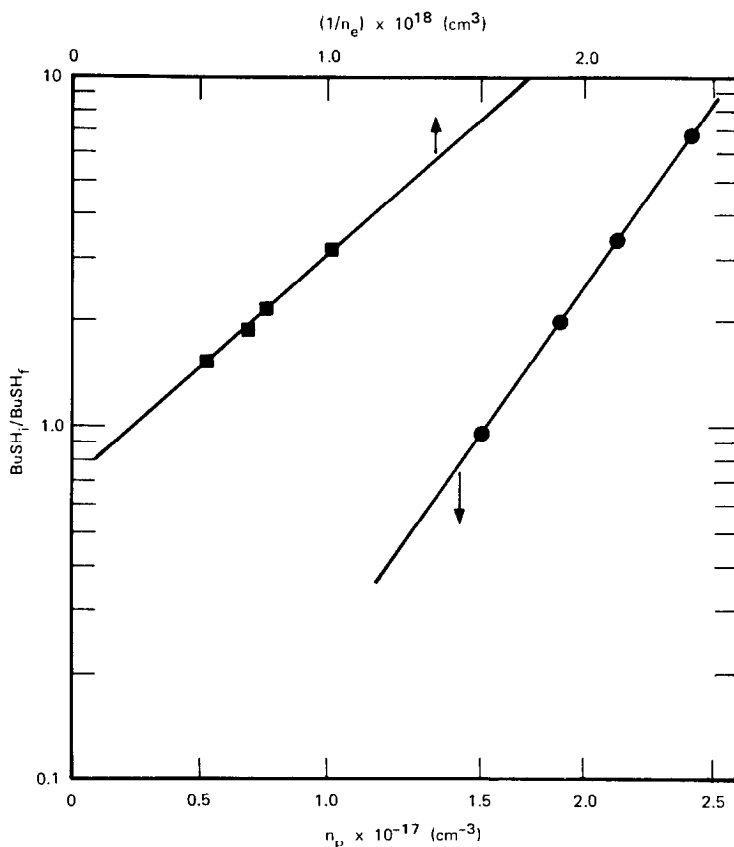


FIG. 2. HDS activity as a function of electronic carrier density.

of  $S^{2-}$  anions or  $Co^{2+}$  cations to the lattice, as observed experimentally. The advantage of  $Co^{2+}$  doping over  $S^{2-}$  addition is to be found in the stabilization of the Fermi level by  $Co^{2+}$ . The  $S^{2-}$  ions are susceptible to reaction with  $H_2$  and their removal or introduction causes a change in the electronic structure of the solid and its catalytic properties. No such problems are encountered with the  $Co^{2+}$ -doped catalyst because the Fermi level is dominated by the foreign cation.

#### REFERENCES

1. Farragher, A. R., and Cossee, P., "Proceedings, Fifth International Congress on Catalysis," Paper No. 94. North-Holland, Amsterdam, 1973.
2. Lipsch, J. M. J. G., and Schuit, G. C. A., *J. Catal.* **15**, 163 (1969).
3. De Beer, V. H. J. *et al.*, *J. Catal.* **27**, 357 (1972).
4. Aoshima, A., and Wise, H., *J. Catal.* **34**, 145 (1974).
5. Kolboe, S., and Amberg, C. H., *Canad. J. Chem.* **44**, 2623 (1966).
6. Verwey, E. J. W. *et al.*, *Philips Res. Rep.* **5**, 173 (1950).
7. van der Pauw, L. J., *Philips Res. Rep.* **13**, 1 (1958).
8. Fivaz, R., *Helv. Phys. Acta* **36**, 1052 (1963).
9. Wentreck, P. R., and Wise, H., *J. Catal.* **45**, 349 (1976).
10. Richardson, J. T., *Ind. Eng. Chem. Fundam.* **3**, 154 (1964).
11. Metcalf, T. B., *Chim. Ind. Gen. Chim. (Milan)* **102**, 1300 (1969).
12. Hoog, H., *J. Inst. Petrol.* **36**, 738 (1950).
13. Fivaz, R., and Moser, E., *Phys. Rev.* **163**, 743 (1967).
14. Putley, E. H., "The Hall Effect," p. 214. Butterworths, London, 1960.